AGU PUBLICATIONS

JGR

Journal of Geophysical Research: Atmospheres

RESEARCH ARTICLE
10.1002/2013JD020148

Key Points:
- H/C ratios of petroleum source rocks fix the total mass of generated petroleum
- Duration of active petroleum generation constrains rate of natural gas venting
- Natural seepage rate for Uinta Basin, Utah, less than 3000 tonne methane/year

Correspondence to:
M. L. Mansfield,
marc.mansfield@usu.edu

Citation:
Mansfield, M. L. (2014), Kerogen maturation data in the Uinta Basin, Utah, USA, constrain predictions of natural hydrocarbon seepage into the atmosphere, *J. Geophys. Res. Atmos.*, *119*, 3460–3475, doi:10.1002/2013JD020148.

Received 9 MAY 2013
Accepted 9 FEB 2014
Accepted article online 12 FEB 2014
Published online 18 MAR 2014

Kerogen maturation data in the Uinta Basin, Utah, USA, constrain predictions of natural hydrocarbon seepage into the atmosphere

Marc L. Mansfield[1]

[1]Bingham Research Center, Utah State University, Vernal, Utah, USA

Abstract Natural seepage of methane from the lithosphere to the atmosphere occurs in regions with large natural gas deposits. According to some authors, it accounts for roughly 5% of the global methane budget. I explore a new approach to estimate methane fluxes based on the maturation of kerogen, which is the hydrocarbon polymer present in petroleum source rocks and whose decomposition leads to the formation of oil and natural gas. The temporal change in the atomic H/C ratio of kerogen lets us estimate the total carbon mass released by it in the form of oil and natural gas. Then the time interval of active kerogen decomposition lets us estimate the average annual formation rate of oil and natural gas in any given petroleum system, which I demonstrate here using the Uinta Basin of eastern Utah as an example. Obviously, this is an upper bound to the average annual rate at which natural gas seeps into the atmosphere. After adjusting for biooxidation of natural gas, I conclude that the average annual seepage rate in the Uinta Basin is not greater than (3100 ± 900) tonne yr^{-1}. This is (0.5 ± 0.15)% of the total flux of methane into the atmosphere over the Basin, as measured during aircraft flights. I speculate about the difference between the regional 0.5% and the global 5% estimates.

1. Introduction

Studies indicate that a substantial amount of fossil methane is reaching the atmosphere without being burned as fuel [*Lowe et al.*, 1988; *Wahlen et al.*, 1989; *Lassey et al.*, 2007; *Neef et al.*, 2010; *Simpson et al.*, 2012; *Peischl et al.*, 2013]. Furthermore, emissions measurements in two petroliferous basins in the western USA indicate that methane flux to the atmosphere is 4% and 9%, respectively, of total natural gas production [*Pétron et al.*, 2012; *Karion et al.*, 2013]. Because methane is a potent greenhouse gas, these studies have implications for global warming. The obvious explanation for all this fossil methane in the air is leakage from natural gas production and distribution. However, many authors have argued that spontaneous, nonanthropogenic venting of natural gas from the lithosphere to the atmosphere is also a contributing factor.

(In the jargon of the petroleum industry, "production" refers to the extraction of fossil fuels from the crust. I follow that usage here. To avoid confusion, I will use terms such as "formation" and "generation," but never "production," to speak of the creation of hydrocarbon fluids in source rocks in the crust.)

For example, *Johnson and Roberts* [2003] suggest that geologic formations in Colorado and Utah, USA, have been leaking natural gas since the early Tertiary. Furthermore, *Etiope and Klusman* [2010] have catalogued ground-to-air methane flux measurements from around the world. Oil production from one of the fields that they catalogued, the Rangely Anticline in western Colorado, began in 1902 in the vicinity of natural seeps [*Spencer*, 1995], and more recently, *Klusman* [2003a, 2003b] reported significant methane fluxes in the same region.

Global extrapolations of regional measurements such as those catalogued by *Etiope and Klusman* [2010] lead to predictions for natural seepage in the neighborhood of tens of teragrams of methane per year (Tg yr^{-1}) [*Kvenvolden et al.*, 2001; *Etiope and Klusman*, 2002, 2010; *Etiope*, 2004, 2005, 2009, 2012; *Kvenvolden and Rogers*, 2005]. Here, I will take 30 Tg yr^{-1} as the consensus value representing these studies. However, these measurements represent only a few petroliferous regions around the globe, and global extrapolations may therefore be questionable. Furthermore, using statistical arguments to be published later, I will show that the regional estimates are very poorly constrained because natural methane seepage is temporally intermittent and spatially variable. For these reasons, better measurements and estimates of natural seepage are called for.

The total annual methane budget is estimated to be in the hundreds of teragrams annually, with 600 Tg yr^{-1} being a consensus value [*Cicerone and Oremland*, 1988; *Fung et al.*, 1991; *Khalil and Rasmussen*, 1994;

Crutzen, 1995; *Stern and Kaufmann*, 1996; *Hein et al*., 1997; *Lelieveld et al*., 1998; *White et al*., 2007; *Adushkin and Kudryavtsev*, 2010; *Kai et al*., 2011]. If both sets of estimates are reasonable, then flux due to natural methane seepage is roughly 5% of the total budget.

In this paper, I formulate an approach to regional estimates of natural seepage based on the chemical composition of oil and gas source rocks. Modern hydrogen-to-carbon atomic ratios in the rocks permit an estimate of the total amount of hydrocarbon fluids that have been generated over time. The geologic moment at which the rocks first began generating these fluids can also be estimated. The ratio of these two estimates gives an estimate of the average annual generation of hydrocarbon fluids by the source rocks, which is, presumably, at least an order-of-magnitude estimate of the current generation rate. (The mass-to-age ratio provides a natural scale for the generation rate at any given time, and the probability is high that the modern rate will be within an order of magnitude of this. A similar argument is used by *Kvenvolden et al*. [2001].) If we assume that the entire petroleum generating system has achieved steady state, with a balance between generation of fluids in the source rocks and loss of fluids to the atmosphere, then the current generation rate equals the rate of flux to the atmosphere. On the other hand, if steady state has not yet been achieved, and hydrocarbon fluids continue to accumulate in the crust, then the current generation rate provides an upper bound to the atmospheric flux rate. Either way, this line of argument helps us determine how much of the leakage could possibly be natural.

As reported below, I predict that natural seepage from one petroliferous basin is probably less than $(0.5 \pm 0.15)\%$ of the total methane flux from that same basin. If a comparable ratio applies to all petroliferous basins, then the 5% global estimates of natural seepage mentioned above are perhaps too high. However, more than anything, the discrepancy points out the difficulties associated with extrapolations from the regional to the global level, and the need for additional study. Below I comment on this discrepancy.

Kerogen is the solid hydrocarbon polymer that forms from organic matter in sediments as these latter are transformed into sedimentary rocks. For example, it is the primary organic constituent of oil shale. During the process of basin formation, such rocks are eventually buried deeply enough that they reach temperatures at which the kerogen begins to decompose thermally, generating both oil and natural gas [*Tissot and Welte*, 1984; *Allen and Allen*, 2005]. Another important degradation pathway is methanogenic biodegradation, which occurs in many petroleum accumulations [*Milkov*, 2011]. As kerogen decomposes, its chemical composition changes. Indeed, the H/C atomic ratio is one of several practical indicators of kerogen maturity. Over time, kerogen becomes richer in carbon because of the correlation between molecular size and H/C ratio in hydrocarbons: The decomposition products, being lighter, carry away excess hydrogen [*Vandenbroucke and Largeau*, 2007]. Therefore, within the kerogen itself is a record of the amount of carbon that has been released over time through decomposition.

I present an analysis of the kerogen found beneath the Uinta Basin of Duchesne and Uintah Counties, Utah, USA; see Figure 1. ("Uinta" and "Uintah" are common alternative spellings.) This is a petroliferous basin covering approximately 2.3×10^4 km^2, bounded to the north and west by the Uinta and Wasatch Mountain Ranges, to the south by the San Rafael Swell and the Uncompahgre Uplift, and to the east by the Douglas Creek Arch. Natural gas and oil source rocks beneath the basin are the Green River and related formations, which formed in lower to middle Tertiary; the Mesaverde Group, which formed during the Upper Cretaceous; and the Mancos Shale, also Upper Cretaceous [*Tissot et al*., 1978; *Anders et al*., 1992; *Fouch et al*., 1992; *Nuccio and Roberts*, 2003].

There is abundant empirical evidence that anthropogenic activities have modified the natural flow of hydrocarbons to the surface. In the early years of the petroleum era, wells were frequently drilled in the vicinity of obvious surface seeps, and production from such wells almost always led to the cessation of seepage. In general, it appears that fossil fuel production relieves formation pressures, which slows or suspends seepage. On the other hand, repressurization of reservoirs by fluid injection is a very common practice, for at least four different purposes: (1) enhanced oil recovery, (2) waste disposal, (3) natural gas storage, and (4) CO_2 sequestration. There are examples of repressurization stimulating leakage [*Horvitz*, 1985; *Araktingi et al*., 1984; *Arp*, 1992; *Jones and Burtell*, 1996; *Tedesco*, 1999; *Bailey and Grubb*, 2006]. In this paper, my aim is to constrain estimates of surface seepage of natural gas in the preindustrial era, before the perturbing effects of anthropogenic activities.

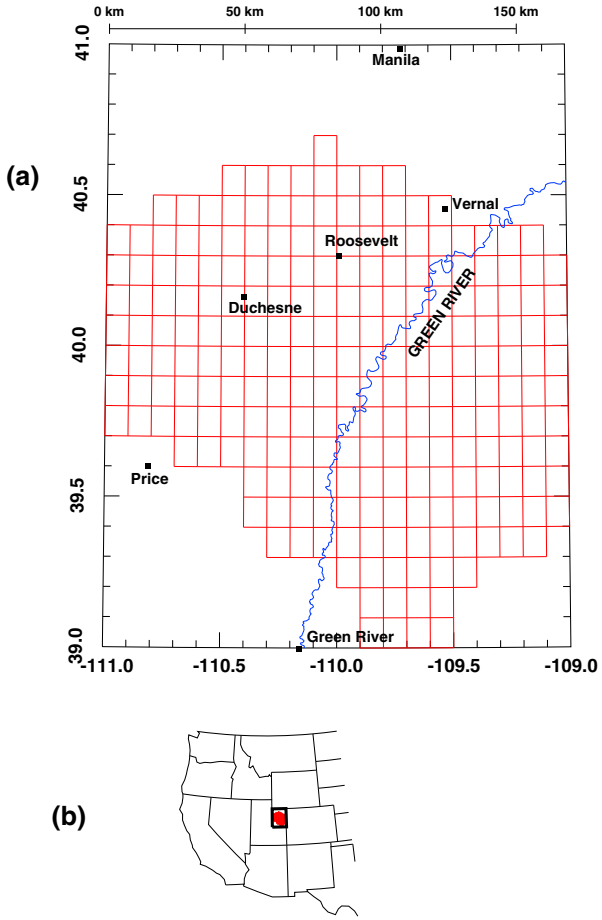

Figure 1. The Uinta Basin of eastern Utah. (a) Regional map, showing the 0.1° × 0.1° integration grid (red), which coincides with the footprint of the basin itself. (b) Location of the basin in the western USA.

Because of discrepancies between different literature data sets, or simply because of a lack of adequate information, it is occasionally necessary to choose between different options as I develop the estimates below. In the interest of arriving at a firm upper bound to the true emission flux, I intentionally resolve such dilemmas so as to maximize the flux estimate. However, I will always point out when such judgments are being made.

The Uinta Basin is one of only two regions worldwide that are known to produce significant atmospheric concentrations of winter ozone [*Schnell et al.*, 2009; *Stoeckenius and Ma*, 2010; *Martin et al.*, 2011; *Lyman and Shorthill*, 2013]. Another purpose of this paper is to determine if natural seepage contributes significantly to ozone precursor emissions in the region.

2. Mechanisms for Natural Gas Seepage

Pore pressures in the lithosphere (i.e., hydrostatic pressure of the fluids found in pores and fractures of the rock) generally obey

$$P_p(z) = g\rho_W(z_s - z) \tag{1}$$

where P_p, g, ρ_W, z_s, and z represent pore pressure, acceleration of gravity, density of water, elevation at the surface, and elevation at depth, respectively. (See Table 1 for a full list of symbols used in this work.) Equation (1) is the pressure-depth relationship expected for any body of water and indicates that any volume element in the water column supports the weight of all the water above. This is significant because it implies that the water in the lithosphere generally forms a continuous phase, in spite of the tortuosity of the pore-fracture-fault network in the crust.

Table 1. List of Symbols Used in This Work

Symbol	Definition
D	Diffusivity
$dV = dx\ dy\ dz$	Volume element within the source rock
f_0	Initial H/C atomic ratio of immature kerogen
f_R	H/C atomic ratio of the hydrocarbons released from kerogen during its maturation
f	Modern H/C atomic ratio of kerogen
F	Initial mass fraction of carbon in source rock; TOC when the rock was immature
g	Acceleration of gravity
G	Geothermal gradient (slope of temperature-depth relationship)
M_R	Total mass of carbon released by kerogen by decomposition
M_T	Total mass of the formation
P_l	Lithostatic pressure
P_p	Pore pressure
$\mathbf{r} = (x, y, z)$	Displacement vector of a position in the formation
R_0	Vitrinite reflectance (an empirical measure of kerogen maturation)
TOC	Total organic carbon of a source rock; mass fraction of the organic carbon in the rock
V_T	Total volume of a formation
x, y, z	Cartesian coordinates: east, north, up, respectively; z measured relative to sea level
z_1, z_2	Elevation of the base and top of the formation, respectively
z_s	Surface elevation
α	Fraction of carbon lost by kerogen during its maturation
$\langle\alpha\rangle$	Mean of α over an entire formation
θ	Celcius temperature
ρ_W, ρ_R	Densities of water and of the source rock, respectively
τ	Time before present at which kerogen decomposition began in a formation
Φ_F	Rate of surface seepage of the carbon mass of hydrocarbons
Φ_R	Rate of release of carbon mass from kerogen
Φ_S	Rate of surface seepage of carbon mass (hydrocarbons plus CO_2)

Lithostatic pressure refers to the stress in the rocks themselves generated by the weight of the overburden. It obeys

$$P_l(z) = g\rho_R(z_s - z) \tag{2}$$

where ρ_R represents the density of the rock. There are conditions under which pore pressure exceeds equation (1). Such formations are said to be overpressured [*Neuzil*, 1995]. However, pore pressure never exceeds lithostatic, because then the fluids are able to relieve stress by fracturing the rock.

Natural gas in the lithosphere can exist in two different physical states, namely, either as a separate gas phase or dissolved in the dominant liquid phase, which is either oil or water. Two mechanisms have been identified that provide for the transport of natural gas in the lithosphere, related to these two physical states.

The fact that the carrier phase of water is continuous provides one of the mechanisms. Natural gas trapped in a reservoir, at partial pressures of hundreds of bars, can dissolve in the water phase and outgas to the atmosphere, where its partial pressure is much less. If the water column is stationary, then transport of dissolved hydrocarbon down the ensuing concentration gradient is governed by Fick's Laws. If the water column circulates in the crust, then transport is even faster, with circulation promoting mixing. The time scale for Fickean transport over a distance Δx is order-of-magnitude equal to $(\Delta x)^2/D$, where D is the diffusivity. D has strong temperature dependence, but in the relevant temperature range, D for methane in bulk water is around 0.1 $km^2\ Myr^{-1}$, or $(\Delta x)^2/D \approx 10$ My if $\Delta x = 1$ km. D for methane in water-saturated solid rock can be from 1 to 3 orders of magnitude smaller, depending on the porosity and permeability of the rock [*Witherspoon and Saraf*, 1965; *Schlömer and Krooss*, 1997; *Sachs*, 1998]. We expect that the effective diffusivity for methane in a water-saturated fracture network lies between the value for bulk water and solid rock. These considerations imply a mega-year to mega-decade time frame for the process. However, we expect the total flux of dissolved gases to depend on the fracture state of the rock column and on water flow patterns, neither of which are well known and both of which vary widely from one petroleum system to another, making it difficult to better constrain the time interval. Nevertheless, it has been asserted that natural gas reservoirs will empty out by dissolution over mega-year time scales, unless they are actively replenished by generation of new gas [*Leythaeuser et al.*, 1982; *Krooss and Leythaeuser*, 1996; *Schlömer and Krooss*, 1997].

Table 2. Results of the Integrations, Equations (4), (6), and (7), for Each of the Formations

Formation	Kerogen Type	f_0	M_T, 10^{18} g	M_R, 10^{18} g	$\langle\alpha\rangle$	τ, Myr	Φ_R, 10^4 tonne/yr
Green River	I	1.6	82	0.60 ± 0.20	10% to 20%	23	2.6 ± 0.9
Mesaverde	III	0.9	33	0.08 ± 0.03	8% to 14%	40	0.20 ± 0.08
Mancos	Mixed II and III	1.1	67	0.20 ± 0.07	10% to 20% (?)	60	0.33 ± 0.11
Total			182	0.88 ± 0.21			3.1 ± 0.9

The other mechanism for natural gas transport might be called "phase invasion," in which natural gas invades the water column as an intact gas phase. Details about the form of the invading phase ("microbubbles" versus plug flow) remain controversial. One major difference between the dissolution and phase invasion mechanisms is the response to pressure. The pressure dependence of the dissolution mechanism is expected to follow Henry's law, i.e., to be linear in the partial pressure of methane in the reservoir. Phase invasion, on the other hand, is expected to be highly nonlinear: An intact second phase cannot leave a reservoir until its pressure is high enough to surmount a capillary barrier. The driving force for transport is gas buoyancy, and ascent times are believed to be on the order of 100 to 1000 m yr^{-1}, much faster than the dissolution mechanism [*Price*, 1986; *Klusman and Saaed*, 1996; *Klusman*, 1997; *Saunders et al*., 1999; *Tedesco*, 1999; *Brown*, 2000].

However, if dissolved natural gas is diffusing away from underground reservoirs, we should ask where, and under what form, it reaches the atmosphere. I pose this question because in many regions, deep crustal water is saline, and if dissolved methane can diffuse away, then certainly electrolytes can also. In fact, because of higher solubility and diffusivity, their transport should be faster. If dissolved methane can reach the surface by this mechanism, then electrolytes should also. However, we all know that groundwater is fresh, not saline. We can resolve this issue by remembering that groundwater is meteoric, and it flows downslope in aquifers, which are nothing more than rock formations with sufficient porosity to permit such flow. When solutes from deeper formations, diffusing slowly upward, encounter the aquifers, we can expect that they become diluted in the faster aquifer flow and that they are carried away by that flow. Because transport of hydrocarbons in solution is inherently slow, and because meteoric water probably contains oxygen and methanotrophic bacteria, it is highly likely that dissolved hydrocarbons are oxidized to CO_2 before they can reach the atmosphere. According to this argument, natural gas bubbling up as an intact gas phase stands a chance of getting through the surface layer of meteoric water, but dissolved natural gas may not.

3. Estimates of Total Carbon Released During Kerogen Decomposition

3.1. Mass Balance Considerations

Assume that a volume of kerogen, which originally contained N_C and N_H carbon and hydrogen atoms, respectively, is later found to contain N_{C1} and N_{H1} atoms, because N_{C2} and N_{H2} atoms of carbon and hydrogen, respectively, have been released through decomposition. Let $f_0 = N_H/N_C$ represent the initial H/C atomic ratio of the immature kerogen, $f_R = N_{H2}/N_{C2}$ that of the hydrocarbons that have been released by decomposition, and $f = N_{H1}/N_{C1}$ that of the mature, remaining kerogen. (The instantaneous f_R ratio depends on the age of the kerogen, since oil and gas are primarily released earlier and later, respectively. However, in the absence of additional data, we are forced to assume that a single f_R value applies throughout the course of maturation.) The two conservation relations $N_C = N_{C1} + N_{C2}$ and $N_H = N_{H1} + N_{H2}$ lead to this relationship

$$\alpha = \frac{N_{C2}}{N_C} = \frac{f_0 - f}{f_R - f} \tag{3}$$

for the fraction of carbon atoms that were released while the kerogen matured to its present state.

Kerogen samples are classified as Types I, II, or III, depending on the ancient depositional environment from which they evolved, and the value of f_0 depends on the kerogen type [*Tissot et al*., 1978; *Vandenbroucke and Largeau*, 2007]. Table 2 summarizes the type classification of Uinta Basin kerogen [*Nuccio and Roberts*, 2003], and the f_0 values that were used in this study [*Anders et al*., 1992; *Nuccio and Roberts*, 2003]. During kerogen maturation, the value of f changes from the f_0 values cited in Table 2 to 0.5 or lower [*Vandenbroucke and Largeau*, 2007]. Precise values of f_R are not known, but we do know that for saturated, acyclic hydrocarbons, it is exactly $2 + 2/n$, where n is the total number of carbon atoms in the molecule. Therefore, it is 4 for methane, 2.67 for propane, 2.25 for octane, and it approaches 2 for large, saturated acyclic hydrocarbons. We also know that both unsaturation and cyclization lead to smaller f_R:

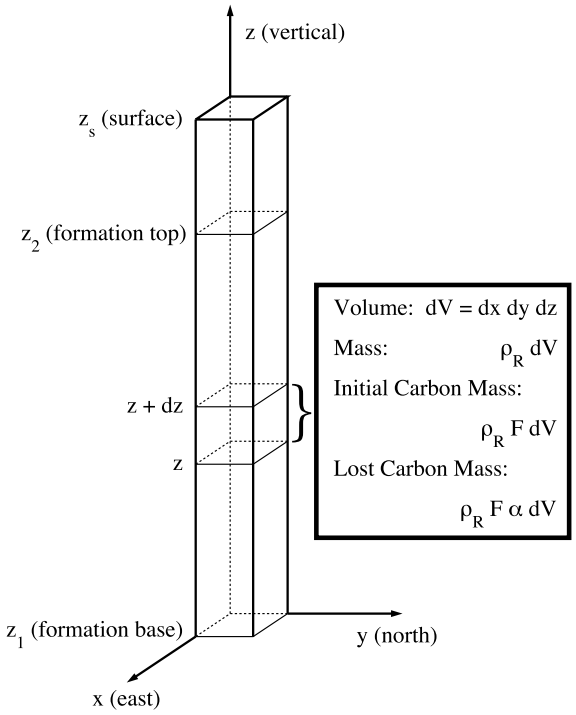

Figure 2. Each grid cell consists of a column extending from the base of the formation, $z = z_1$, to the top, $z = z_2$. An element of volume, dx dy dz, is also shown. Its total mass, the initial mass of carbon, and the mass of carbon lost from its kerogen as a result of decomposition are also displayed.

For example, it is 1 and 0, respectively, for benzene and graphite. We also know that it must be greater than f_0, since α in equation (3) cannot be greater than 1. Uinta Basin crude oil has a high paraffin content [*Tissot and Welte*, 1984, p. 420], which argues for a value nearer to 2, but the basin also produces considerable natural gas, which argues for a value nearer to 4. In this paper, I assume that the appropriate value lies between the extremes of 2 and 4.

Immature kerogen also contains some oxygen, most of which leaves during decomposition as CO_2 [*Tissot and Welte*, 1984]. Because my analysis assigns all missing carbon to oil and natural gas, it probably slightly overestimates the amount of carbon leaving in the form of hydrocarbon.

Consider a volume element within the source rock having volume $dV = dx\,dy\,dz$ at the position $\mathbf{r} = (x,y,z)$, as shown in Figure 2. The x and y coordinates are horizontal, east and north, respectively, while z measures the altitude relative to sea level. The volume element has mass $\rho_R\,dV$, where $\rho_R \approx 2.4\ \mathrm{g\ cm^{-3}} = 2.4\ \mathrm{Pg\ km^{-3}}$ is the density of the rock. The mass fraction of carbon within such rocks is a ratio known as the total organic carbon, or TOC. TOC refers to carbon found not only in the insoluble kerogen but also in bitumen, the soluble organic component of the rock. Bitumen consists of lower hydrocarbons which have been separated from the kerogen by decomposition, but which have not yet been expelled from the source rock. Here, we let $F(\mathbf{r})$ represent the total mass fraction of carbon in the rock when it still contained only immature kerogen, i.e., its initial TOC value. With these definitions, the total mass of carbon found initially in the kerogen in the volume element dV is $\rho_R F(\mathbf{r})\,dV$, while the net mass of carbon to have been released from the kerogen over time is $\rho_R F(\mathbf{r})\alpha(\mathbf{r})\,dV$. We let V_T represent the total volume of the formation, and we integrate $\rho_R F(\mathbf{r})\alpha(\mathbf{r})\,dV$ over the entire volume to determine the net mass of released carbon, M_R. The function α appears with $\mathbf{r}$ dependence since, as already pointed out, deeper rocks have spent more time in the temperature window for thermal decomposition and therefore have released more carbon. F also appears as a function of $\mathbf{r}$ because it can vary considerably from one point to another in a formation [*Law*, 1984; *Creany and Passey*, 1993]. Technically speaking, ρ_R is also a function of $\mathbf{r}$, but its variability is low, and so is treated as a constant. We obtain

$$M_R = \rho_R \int_{V_T} \alpha(\mathbf{r}) F(\mathbf{r})\ d\mathbf{r} = \rho_R \int_{V_T} \left[\frac{f_0 - f(\mathbf{r})}{f_R - f(\mathbf{r})}\right] F(\mathbf{r})\ d\mathbf{r} \tag{4}$$

In the above,

$$\int_{V_T} g(\mathbf{r})\,d\mathbf{r} \tag{5}$$

is our notation for integrating an arbitrary function $g(\mathbf{r})$ over the volume of the formation. In this notation, the total mass of the formation may be written as

$$M_T = \rho \int_{V_T} d\mathbf{r} = \rho V_T \tag{6}$$

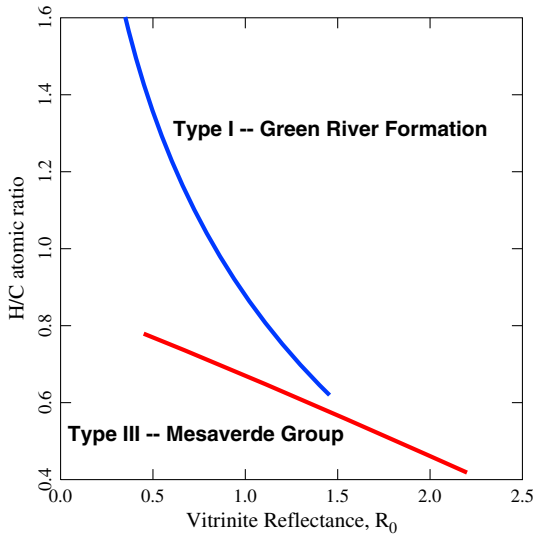

Figure 3. Empirical correlations between H/C atomic ratio and vitrinite reflectance employed in this work for kerogen Types I and III. The curves correspond to equations (8) and (13), respectively.

As a measure of the overall maturity of the source-rock formation, we also calculate the mean of α over the entire volume:

$$\langle \alpha \rangle = \frac{1}{V_T} \int_{V_T} \alpha(\mathbf{r}) \; d\mathbf{r} \tag{7}$$

The integrals shown in equations (4), (6), and (7) were performed numerically with a resolution of 0.1° longitude by 0.1° latitude in the x and y variables, respectively, which defines the grid system shown in Figure 1. Each individual grid cell consists of a rectangular column extending from $z = z_1$ to $z = z_2$, as shown in Figure 2, representing respectively the altitudes at the base and the top of the formation. For each grid cell, we also define $z = z_s$ as the altitude of the surface. The values of z_1, z_2, and z_s are assumed to be constant throughout an individual cell and are assigned as explained below. Obviously, in each cell we have $z_s \geq z_2 \geq z_1$. The integrals along z within each grid cell extend from z_1 to z_2 and were performed by trapezoidal rule integration. Within any one grid cell, $\alpha(\mathbf{r})$ is assumed to be a function of z and z_s, as explained below. At the latitude of the Uinta Basin, the cross-sectional area, A, of each grid cell is 94.7 km^2, and 232 grid cells are required to cover the basin.

The literature contains other calculations of the total hydrocarbon mass released by kerogen in other petroleum systems [*Cooles et al.*, 1985; *Pepper and Corvi*, 1995a, 1995b; *Pepper and Dodd*, 1995]. As far as I know, the current contribution is novel in its use of carbon and hydrogen mass balances to arrive at estimates of M_R.

3.2. Contribution From the Green River and Related Tertiary Formations

Because of differences in the way that maturation data have been reported in the literature, it is convenient to consider each formation independently. We begin with the Green River and related Tertiary formations [*Tissot et al.*, 1978; *Anders et al.*, 1992; *Fouch et al.*, 1992; *Nuccio and Roberts*, 2003], and results for all three formations are summarized in Table 2.

Values of z_1 and z_2 in each grid cell were assigned based on data from *Fouch et al.* [1992, Figure 14] and *Anders et al.* [1992, Figure 2]. Values of z_s were assigned using elevation data from Google Earth.

Kerogen maturation data for the Green River Formation beneath the Uinta Basin have been obtained from core samples and are reported by *Anders et al.* [1992]. However, much of these are actually in the form of another maturation indicator, the so-called vitrinite reflectance index, or R_0 [*Vandenbroucke and Largeau*, 2007]. Fortunately, *Anders et al.* [1992, Figure 6] also provide the following correlation between R_0 and f:

$$f = 0.8785 - 1.587 \;\; \log_{10} R_0 \tag{8}$$

Equation (8) appears plotted in Figure 3.

Kerogen maturation varies with the depth, $z_s - z$, of the sample. I have been unable to find a direct relationship between R_0 and depth, but the paper of Anders *et al.* [1992] provides enough information to formulate one. They identify four stages in the kerogen aging process: onset of oil production, peak in oil production, end of intense catagenesis, and end of liquid hydrocarbon preservation; they associate both temperature (95°C, 110°C, 135°C, and 150°C) and vitrinite reflectance (0.7, 0.9, 1.2 and 1.4%) with each stage. These four data points all lie essentially on the line

$$R_0 = -0.4938 + \frac{\theta}{79.37 \;\; ^\circ\mathrm{C}} \tag{9}$$

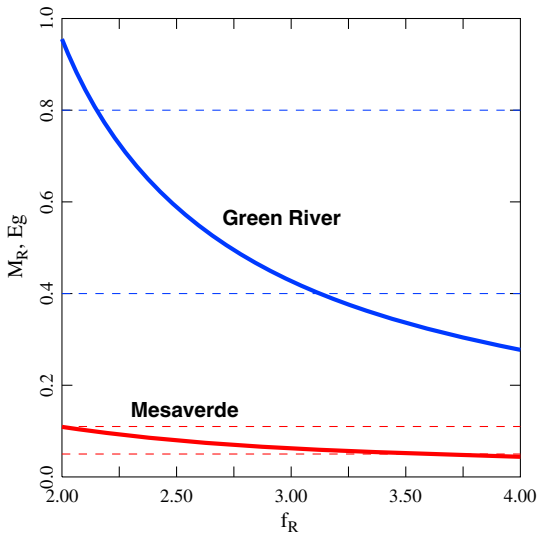

Figure 4. M_R is the total mass of carbon lost by a formation over its lifetime and is calculated as a function of the variable f_R. The dashed lines define the respective ranges, 0.6 ± 0.2 Eg and 0.08 ± 0.03 Eg, used in subsequent work.

where θ represents the Celcius temperature. We will use equation (9) to relate R_0 to θ. Furthermore, over relevant depths within the upper crust, it is appropriate to assume linearity between depth and temperature:

$$\theta = G(z_s - z) + 25°\text{C} \qquad (10)$$

where $z_s - z$ represents depth below the surface. G is the so-called geothermal gradient, which varies from about 11 to 38 °C/km between the north and the south of the basin. G was taken to be constant within each grid cell, and the values for each grid cell are obtained from *Anders et al.* [1992, Figure 9].

Using equations (8)–(10), we are able to estimate $f(z)$, i.e., the H/C atomic ratio as a function of altitude in each grid cell, which then gives $\alpha(z)$ according to equation (3). However, a slight modification is still required. The above formulas have been developed for the window of active decomposition and are inappropriate at shallower depths. The symptoms of the problem are either a negative R_0 or a negative α, both of which are physically meaningless. To avoid this problem, we assume that α is exactly zero at any of the shallow depths for which the above formulas produce either the condition $R_0 < 0$ or $\alpha < 0$.

A significant source of uncertainty in these calculations is the value of $F(\mathbf{r})$. As mentioned above, F is equal to the initial value of total organic carbon (TOC), expressed as a mass fraction. TOC values fluctuate widely with depth in a single core sample and from core to core in a given formation [*Creany and Passey*, 1993]. Therefore, an appropriate $F(\mathbf{r})$ is difficult to ascertain, and a common practice in basin modeling is to apply a constant, coarse-grained average value throughout a formation, but because of high variability in the measurements, even that is difficult to determine accurately [*McPherson*, 1996]. Furthermore, we are interested in an initial, ancient value, before the sample lost any carbon to decomposition. Also, modern TOC numbers include contributions from both kerogen and bitumen in the rock, whereas H/C or vitrinite reflectance data apply only to kerogen. This fact would complicate any effort to project an initial TOC based on the difference between $f(\mathbf{r})$ and f_0. Worldwide, TOC values are cited to lie in the range of a few percent [*Allen and Allen*, 2005]. However, the upper portions of the Green River Formation are exceptionally rich in carbon. For example, *Tissot et al.* [1978] present TOC measurements in the range of 1% to 20%, with a few samples reaching as high as 60%. Other measurements for this formation are at similar values [*Bredehoeft*, 1998; *McPherson*, 1996]. However, an average of 3% is reported for a core taken in the lower part of the formation [*Wiggins and Harris*, 1994]. The overall trend in TOC appears to be from high to low with increasing depth [*Tissot et al.*, 1978]. The approach used here is to assume that $F(\mathbf{r})$ is 12% at the top of the formation ($z = z_2$) and 2% at the base ($z = z_1$) and that it varies linearly at all other z. As explained below, this gives an effective F throughout the formation of about 3%. This is larger than the coarse-grained average (1.6%) used in another study of the Green River Formation [*McPherson*, 1996] but will be used here because of my stated intention to overestimate. Since equation (4) is proportional to F, all results reported below are subject to a similar uncertainty.

For the Green River Formation beneath the Uinta Basin, the above procedure yields $V_T = 3.4 \times 10^4$ km^3 and $M_T = 82$ Eg. Computation of M_R and $\langle\alpha\rangle$ depends on the poorly constrained f_R. Figures 4 and 5 show how M_R and $\langle\alpha\rangle$ vary with f_R. As asserted above, f_R certainly lies between 2 and 4. However, the likelihood that it lies near either 2 or 4 is small. Therefore, I have chosen to use, for the probable range of both M_R and $\langle\alpha\rangle$, the mean ± 1 standard deviation as f_R varies between 2 and 4. Therefore, I assume the ranges $M_R = (0.6 \pm 0.2)$ Eg and $\langle\alpha\rangle = (15 \pm 5)\%$ for this formation. Figure 6 displays by gray scale the contribution of each grid cell to the total mass M_R, using as an example $f_0 = 1.6$ and $f_R = 2.5$. The cells that have lost the most carbon lie along the northern flank of the basin where the formation is most deeply buried.

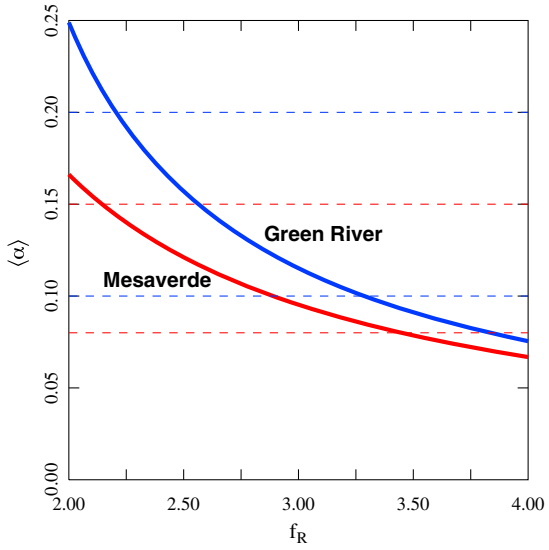

Figure 5. $\langle\alpha\rangle$ represents the fraction of carbon lost from each formation over its lifetime and is calculated as a function of f_R. The dashed lines define the respective ranges, 0.15 ± 0.05 and 0.11 ± 0.03, applied in subsequent steps.

Let Φ_R represent the average annual release rate of carbon from the kerogen in any given formation. It can be estimated by dividing the total mass of released carbon by the period of time, τ, over which the release occurred:

$$\Phi_R = \frac{M_R}{\tau} \quad (11)$$

Estimates of τ for the Green River Formation beneath the Uinta Basin are variously put at 40 Myr [*Bredehoeft*, 1998] and at 23 Myr [*Nuccio and Roberts*, 2003]. As explained above, I resolve this dilemma using the value, τ = 23 Myr, which maximizes the final result, appreciating that the choice of 23 over 40 Myr produces a nearly twofold increase in the final estimate:

$$\Phi_R \approx (2.6\pm0.9) \times 10^4 \text{ tonne yr}^{-1} \quad (12)$$

3.3. Contribution From the Mesaverde Group

We next estimate the contribution from the older Mesaverde Group. It is more inhomogeneous than the Green River Formation, containing both coal seams and noncarbonaceous sandstones [*Johnson and Roberts*, 2003]. The coal seams are expected to be a very rich source of methane, but accounting for them correctly would require a more detailed analysis. Fortunately for our estimates, the Group is dominated by the carbonaceous shales, and we will assume that contributions from the coal and noncarbonaceous sandstone deposits are largely compensatory. Once again, an appropriate *F* value is probably the single largest uncertainty in our estimate. Shale TOC values for the Almond Formation of the Mesaverde Group in southwestern Wyoming are reported in the range of 0.2% to 19.1% [*MacGowan et al.*, 1992], similar to ranges reported above for the Green River Formation. Although TOCs approaching 20% or more occur in these source rocks, the averages are probably much lower. For example, TOCs sampled from Upper Cretaceous source rocks in the Greater Green River Basin of Wyoming are also reported to lie in a range from around 0% to around 20%, but with an average of 2% [*Law*, 1984]. I have been unable to find TOC measurements for the Mesaverde Group of the Uinta Basin. However, all the Wyoming source rocks listed above

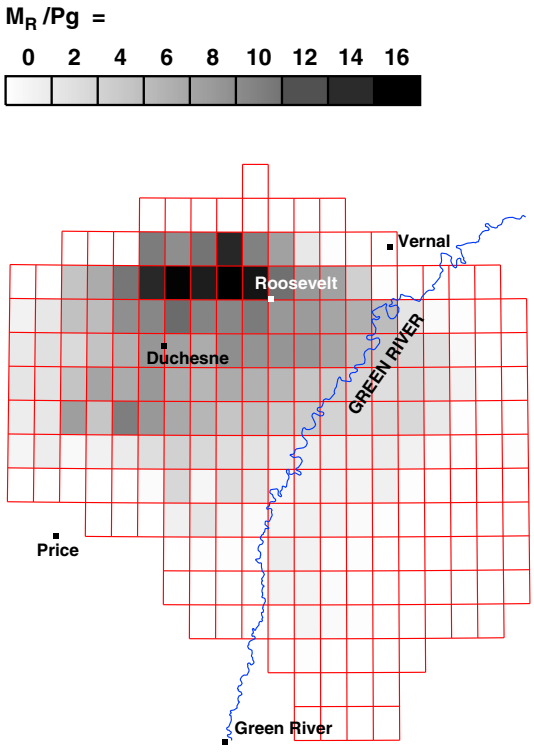

Figure 6. Estimated mass of carbon released in each grid cell by the Green River and related formations.

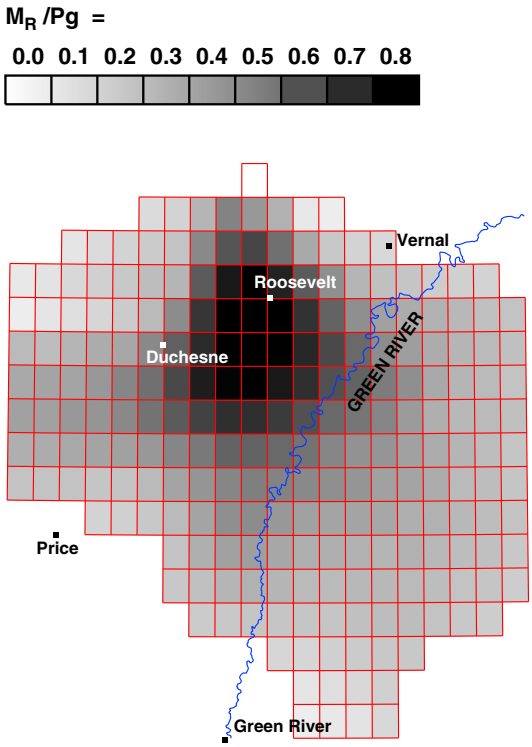

Figure 7. Estimated mass of carbon released in each grid cell by the Mesaverde Group.

are correlative with the Mesaverde Group of the Uinta Basin; hence, I assume $F = 0.02$ for the entire Group.

Depth data for this formation were obtained from *Fouch et al.* [1992, Figure 16] Kerogen maturation data are available as R_0 reported at the base ($z = z_1$) and at the top ($z = z_2$) of the formation [*Nuccio et al.*, 1992, Figures 4 and 5]. At all other depths z, with $z_1 < z < z_2$, we assume that R_0 varies linearly between z_1 and z_2. Equation (8) above only applies to Type I kerogen, while the Mesaverde Group is reported to contain Type III [*Nuccio and Roberts*, 2003]. An appropriate analogue to equation (8) for Type III kerogen is

$$f = 0.86 - 0.19 R_0^{1.07} \tag{13}$$

which was adapted from *Tissot and Welte* [1984, p. 161]. Equation (13) is also plotted in Figure 3.

We obtain $V_T = 1.4 \times 10^4$ km^3 and $M_T = 33$ Eg. Figure 4 shows how M_R varies with the assumed value of f_R. Consistent with Figure 4, I employ the range $M_R = (0.08 \pm 0.03)$ Eg. As shown in Figure 5, the appropriate range for $\langle\alpha\rangle$ is 8% to 14%. Figure 7 shows the mass contributions by grid cell, under the assumptions $f_0 = 0.9$ and $f_R = 2.5$. For this formation, I assume $\tau = 40$ Myr [*Nuccio and Roberts*, 2003] and obtain

$$\Phi_R \approx (2.0 \pm 0.8) \times 10^3 \text{ tonne yr}^{-1} \tag{14}$$

There are essentially two reasons that M_R for this formation is considerably lower than that for the Green River. First, the overall bulk of the two formations, as measured by the respective M_T, differs by a factor of about 2.5. Second, Type III kerogen is less productive than Type I. This is obvious, for example, in equation (3): α is larger when f is nearer to f_R.

3.4. Contribution From Mancos Shale

I have been unable to find depth data on the Mancos Shale beyond the statement that it is 4000 ft (1.2 km) thick on average beneath the Uinta Basin [*Ressetar*, 2012], which implies $V_T = 2.8 \times 10^4$ km^3 and $M_T = 67$ Eg. However, based on results for the previous two formations, it is still possible to make an estimate. R_0 data are available [*Quick and Ressetar*, 2012; *Nuccio and Roberts*, 2003] and indicate the greater maturity of these source rocks. Because it is mixed Types II and III [*Nuccio and Roberts*, 2003], and because it is more mature, its $\langle\alpha\rangle$ should be at least as large as that of the Mesaverde Group. For purposes of estimation, I will assume that $\langle\alpha\rangle$ is in the range of 10% to 20%. Measured TOC values are in the 1% to 2% range [*Anderson and Harris*, 2006; *Schamel*, 2005, 2006]. Therefore, I use the estimate $F = 0.02$. Then rather than performing the actual integral, I assume $M_R \approx F\langle\alpha\rangle M_T \approx (0.20 \pm 0.07)$ Eg. I also assume the value $\tau = 60$ Myr [*Nuccio and Roberts*, 2003], obtaining the estimate

$$\Phi_R = (3.3 \pm 1.1) \times 10^3 \text{ tonne yr}^{-1} \tag{15}$$

4. Average Annual Release of Carbon From Kerogen

Summing the contributions of the three formations, equations (12), (14), and (15), gives

$$\Phi_R = (3.1 \pm 0.9) \times 10^4 \text{ tonne yr}^{-1} \tag{16}$$

Inasmuch as Φ_R represents the average mass of carbon released each year by kerogen decomposition, I will also assume that it is an approximate estimate for the release rate in modern times, but prior to the onset of the petroleum era.

Nuccio and Roberts [2003] assert that kerogen decomposition in the Mancos Shale effectively stopped several million years ago. Therefore, one option is to remove its contribution, arriving thereby at a slightly smaller estimate. However, natural gas from the Mancos Shale is obviously still present underground. Perhaps a better estimate can be achieved by retaining its contribution. In any case, true to the intention stated above, to resolve such dilemmas by maximizing the estimate, I will use the 3.1×10^4 tonne yr^{-1} estimate in what follows.

5. Arguments Based on Steady State Conditions

Let Φ_S represent the average annual surface seepage, i.e., the annual carbon flux through the surface of the Earth. We also expect $\Phi_S \leq \Phi_R$. Equality, $\Phi_S = \Phi_R$, will hold if the entire petroleum system is in steady state. Under this assumption, on any given year, the number of carbon atoms freed from kerogen by decomposition is balanced by an equal number of carbon atoms venting to the atmosphere, and there is no net accumulation of carbon between the source (kerogen) and the sink (the atmosphere). The inequality, $\Phi_S < \Phi_R$, will hold if the system has not yet reached steady state, but rather carbon released by kerogen decomposition is still accumulating underground.

The notion that many hydrocarbon reservoirs are at steady state, with gains balanced by losses, is not new. For example, the Hobson-Berg equation successfully estimates the size of many conventional oil and gas reservoirs by assuming, first, that a reservoir has a limited capacity determined by a capillary barrier between it and an overlaying formation and, second, that such a reservoir is already filled to capacity [*Berg*, 1975; *Allen and Allen*, 2005, p. 448]. If already filled, then one drop of oil or gas leaves for every drop that enters.

Steady state arguments have also been invoked relative to the dissolution mechanism discussed in section 2. It is believed that many natural gas reservoirs lose gas to solution in the water column as rapidly as new gas arrives [*Leythaeuser et al*., 1982; *Saunders et al*., 1999].

However, it is one thing to assert that a single reservoir is in steady state and another that an entire petroleum system is. Many natural gas reserves in the Uinta Basin and elsewhere are in "tight sand" formations, i.e., low-permeability sandstone. *Law* [1984] asserts that gas migration is not greater than a few hundred feet (a few thirties of meters) in tight gas rocks. The regions of high hydrocarbon generation in Figure 6 are overpressured, and most researchers believe that these high pressures are the result of on-going natural gas generation and accumulation in these formations [*Bredehoeft*, 1998; *Bredehoeft et al*., 1994; *McPherson and Bredehoeft*, 2001; *Neuzil*, 1995; *Spencer*, 1987]. Therefore, since it seems likely that natural gas continues to accumulate, the basin is not in steady state, and therefore, $\Phi_S < \Phi_R$:

$$\Phi_S < (3.1 \pm 0.9) \times 10^4 \ \text{tonne yr}^{-1} \tag{17}$$

The relative magnitudes of Φ_S and Φ_R depend on the balance between accumulation in the lithosphere and transmission to the atmosphere and are difficult to predict at this time.

Furthermore, the steady state argument probably applies only to the preindustrial period. Oil and gas production from these formations, coupled with artificial reinjection of fluids into the formations, has no doubt disturbed any steady state that might have been established previously. Total natural gas production for 2012 from the two counties equals 7.1×10^6 tonne yr^{-1} [*Utah Division of Oil, Gas, and Mining* (*UDOGM*), 2013], which is over 200 times larger than equation (17), bolstering the assertion that production has disturbed any previously established steady state. On the other hand, it is now common practice to repressurize reservoirs by fluid injection. Therefore, equation (17) probably only applies to the preindustrial era, and modern flow rates are more difficult to constrain.

6. Bacterial Methanotrophy and Methanogenesis

In water and soil near the earth's surface, methanotrophic bacteria are expected to oxidize much of the natural gas to CO_2 [*Op den Camp et al*., 2009; *Joye*, 2012; *Milucka et al*., 2012]. It has been asserted that 90% of the methane approaching the surface is turned over by methanotrophs in this way [*Etiope*, 2005]. Most of the

research to date applies to biooxidation of methane; however, butane eaters are also mentioned in the literature [*Zhang et al*., 2012]. In section 2 above, I argued that natural gas ascending in solution, since it travels more slowly, might well be completely oxidized and never reach the atmosphere.

As mentioned above, another important process is anaerobic biodegradation of higher hydrocarbons to methane, which occurs in many petroleum reservoirs [*Milkov*, 2011]. However, this process can be thought of as an additional step in the overall decomposition of kerogen and so does not affect the calculations presented here.

There is evidence that methanotrophy is suppressed in winter [*Klusman et al*., 2000; *Klusman and Dick*, 2000; *Klusman*, 2003a, 2003b]. This is relevant for two reasons. First, it means that year-round flux measurements are required to estimate annual fluxes in temperate regions, and second, it means that emissions affecting the winter ozone phenomenon in the Uinta Basin are seasonally larger than their annual rates.

Assuming the 90% loss rate mentioned above, and letting Φ_F represent the annual atmospheric flux of natural gas surviving biooxidation, we arrive at this upper bound for the annual flux rate:

$$\Phi_F < (3100 \pm 900) \text{ tonne yr}^{-1} \tag{18}$$

7. Summary

The calculation detailed above will now be summarized, step by step, combining contributions from all three formations, ignoring uncertainty estimates, but summarizing sources of uncertainty in each step. In order to combine contributions from all three formations, it is also necessary to apply approximate, blended values of the multipliers $\langle F \rangle$, $\langle \alpha \rangle$, and $1/\tau$.

Step 1: The total volume of source rock is

$$V_T = 76 \times 10^3 \text{ km}^3 \tag{19}$$

Step 2: Multiply (19) by the rock density, 2.4×10^9 tonne km^{-3}, to obtain the total mass of source rocks:

$$M_T = 182 \times 10^{12} \text{ tonne} \tag{20}$$

Step 3: Multiply (20) by $\langle F \rangle \approx 3\%$ to obtain the carbon mass of the source rocks prior to kerogen decomposition:

$$5.5 \times 10^{12} \text{ tonne} \tag{21}$$

Uncertainty accumulates at this step for two reasons. First, modern total organic carbon (TOC) values are highly variable throughout a formation, so it is uncertain whether existing measurements are truly representative. Second, for obvious reasons we are only able to measure modern TOCs, whereas initial, ancient values are desired.

Step 4: Multiply (21) by $\langle \alpha \rangle \approx 16\%$ to obtain the total mass of carbon released from kerogen by decomposition:

$$M_R = 880 \times 10^9 \text{ tonne} \tag{22}$$

Uncertainty in this step results because f_R is poorly constrained; see Figures 4 and 5.

Step 5: Divide (22) by the time interval over which decomposition has been occurring in the source rocks, $\tau \approx 3 \times 10^7$ y, obtaining the average annual rate of carbon release by decomposition:

$$\Phi_R = 29 \times 10^3 \text{ tonne yr}^{-1} \tag{23}$$

Uncertainty in this step devolves from the timing of the initiation of decomposition. As mentioned above, τ for the Green River Formation is placed variously at 23 Myr and 40 Myr.

Step 6: Equation (23) represents an average rate over many million years, but we then assume it also approximates the modern, preindustrial rate. This generates still more uncertainty. Because of recent basin uplift, it has been argued that the decomposition rate under the basin has subsided somewhat during the last few million years [*Nuccio and Roberts*, 2003]. This would imply that the estimate in this step is high.

Step 7: Under steady state conditions, the rate of carbon release from kerogen would be balanced by the rate of carbon flux to the atmosphere. However, as explained above, it seems unlikely that the entire basin is in steady state. Therefore, the rate of carbon flux to the atmosphere must be less than (23):

$$\Phi_S < 29 \times 10^3 \text{ tonne yr}^{-1} \quad (24)$$

Uncertainty accumulates here because, although I am confident in saying that Φ_S must be less than Φ_R, I frankly cannot say how much less.

Step 8: Methanotrophs convert some portion of the natural gas into CO_2. Following *Etiope* [2005], we reduce (24) by an order of magnitude:

$$\Phi_F < 2900 \text{ tonne yr}^{-1} \quad (25)$$

Uncertainty accumulates here because the exact loss to methanotrophy is unknown.

Equations (18) and (25) are essentially equal, because of the uncertainty appearing in the former.

8. Discussion and Conclusions

It is informative to compare the above estimates with other emissions data and measurements. For example, one emissions inventory [*Bar-Ilan et al*., 2009] estimates that the total nonmethane hydrocarbon emission attributable to the oil and gas industry of Uintah and Duchesne Counties was 6.0×10^4 tonne yr^{-1} in 2006. Equation (18) is (5.0 ± 1.5)% of that amount. Typical natural gas produced from the Green River Formation of the Uinta Basin ranges between about 76 and 98 mol % methane, with most samples being around 95% [*Zhang et al*., 2009]. Therefore, on the order of 10% of the carbon mass accounted for in Φ_F appears as nonmethane hydrocarbon, i.e., not more than about 300 tonne yr^{-1} or less than 0.5% of the 2006 emissions estimate. Nonmethane hydrocarbons are important ozone precursors, and as mentioned above, the Uinta Basin is one of two regions worldwide known to produce high winter ozone concentrations. The present calculation indicates that natural gas seepage is probably not a significant contributor to this ozone production.

Total natural gas production for the two counties in 2012 was 7.1 Tg yr^{-1} [*UDOGM*, 2013]. This figure is 230 times larger than equation (17). In other words, anthropogenic extraction rates far exceed estimated annual rates due to natural seepage. This reinforces the belief that modern extraction of fossil fuels has disrupted any steady state process that might have existed prior to the industrial era.

Total cumulative production (through the end of 2012) from the two counties is 89.6 Tg of natural gas and 88.1 Tg of oil [*UDOGM*, 2013]. Twenty years ago, total estimated recoverable reserves of oil in the Green River and related formations were put at 100 Tg [*Fouch et al*., 1992]. The total estimated amount of natural gas in place in the Wasatch Formation is 400 Tg, of which about 110 Tg were considered recoverable 20 years ago [*Fouch et al*., 1992]. (Above we referred to the Green River and "related" formations; the Wasatch is one of the formations related to the Green River.) All these quantities, in the vicinity of 100 Tg, are miniscule in comparison to the above estimate which puts M_R for the Tertiary formations at 600,000 Tg. Of course, M_R includes not only gas and oil that have been expelled from the source rocks, but bitumen still trapped in the source rocks, which could account for much of the discrepancy.

Aircraft measurements of methane emissions conducted during February 2012 in the Uinta Basin lead to the estimate that an amount equal to about 9% of the total natural gas production of 7.1 Tg yr^{-1}, or about 6×10^5 tonne yr^{-1}, enter the atmosphere [*Karion et al*., 2013]. Equation (18) is (0.5 ± 0.15)% of that figure. The 6×10^5 tonnes are predominantly fossil methane: Estimates of emissions by ruminants are only 5.0×10^3 tonne yr^{-1} [*Lyman and Shorthill*, 2013], and no other significant industrial, biogenic, or agricultural sources are expected to be active in February. Furthermore, other hydrocarbons sampled during the flights follow the signature expected of emissions by the oil and gas industry [*Karion et al*., 2013].

An estimate of about 0.5% is problematic because, as mentioned in section 1, a number of authors put the global contribution due to natural seepage at roughly 5% of *all* methane emissions, fossil, and nonfossil. I can offer several explanations for the discrepancy:

1. The global estimates are poorly constrained. The authors of all the relevant studies concur with *Kvenvolden et al*. [2001], who state that "these are first approximations to be refined as more information

is obtained." The studies involve extrapolations from a relatively small number of petroliferous basins, without regard to whether individual reservoirs are conventional or unconventional, deep or shallow, or the extent to which fluids are currently being extracted or injected.

2. As already mentioned, natural gas reservoirs beneath the Uinta Basin are deep and tight. Perhaps its seepage is not representative of contributions worldwide.
3. As already mentioned, the arguments contained herein apply more accurately to the preindustrial era, before the production and reinjection of fluids in petroliferous basins. Today, perhaps the best places to look for seepage are over reservoirs that have been artificially repressurized. Presumably, formations selected for reinjection tend to be more shallow and therefore may be more prone to surface leakage, and obviously we can assume that some of the seepage measurements cataloged by *Etiope and Klusman* [2010] were taken at such sites.

Acknowledgments

I express appreciation to Benjamin Burger, Department of Geology, Utah State University, for reviewing and commenting on the manuscript. This research was funded by the Uintah Impact Mitigation Special Services District, Uintah County, Utah, USA, and by the Utah Science Technology and Research Initiative.

References

Adushkin, V. V., and V. P. Kudryavtsev (2010), Global methane flux into the atmosphere and its seasonal variations, *Izvestiya, Phys. Solid Earth*, *46*, 350–357, doi:10.1134/S1069351310040075.

Allen, P. A., and J. R. Allen (2005), *Basin Analysis: Principles and Applications*, 2nd ed., Blackwell, Oxford.

Anders, D. E., J. G. Palacas, and R. C. Johnson (1992), Thermal maturity of rocks and hydrocarbon deposits, Uinta Basin, Utah, in *Hydrocarbon and Mineral Resources of the Uinta Basin, Utah and Colorado: Utah Geological Association Guidebook 20*, edited by T. D. Fouch, V. F. Nuccio, and T. C. Chidsey Jr., pp. 53–76, Utah Geological Association, Salt Lake City, Utah.

Anderson, D. S., and N. B. Harris (2006), Integrated sequence stratigraphic and geochemical resource characterization of the lower Mancos Shale, Uinta Basin, Utah, *Open File Rep., 483*, Utah Geological Survey, Utah Department of Natural Resources, Salt Lake City, Utah.

Araktingi, R., M. Benefield, Z. Bessenyei, K. Coats, and M. Tek (1984), Leroy storage facility, Uinta County, Wyoming: A case history of attempted gas-migration control, *J. Pet. Technol.*, *34*, 132–140.

Arp, G. K. (1992), An integrated interpretation for the origin of the Patrick Draw Oil Field sage anomaly, *Am. Assoc. Pet. Geol. Bull.*, *76*, 301–306.

Bailey, T. C., and J. M. Grubb (2006), Drilling confirms radar-mapped atmospheric seepage anomalies, *Oil Gas J.*, *104*, 32–37.

Bar-Ilan, A., R. Friesen, R. Parikh, J. Grant, A. K. Pollack, D. Henderer, D. Pring, and K. Sgamma (2009), Development of 2012 oil and gas emissions projections for the Uinta Basin, Environ, Novato, California, USA. [Available at http://wrapair.org/forums/ogwg/documents/2009-03_12_Projection_Emissions_Uinta_Basin_Technical_Memo_03-25.pdf.]

Berg, R. R. (1975), Capillary pressure in stratigraphic traps, *Am. Assoc. Pet. Geol. Bull.*, *59*, 939–956.

Bredehoeft, J. D. (1998), Final report on Grant DE-AI03-93-ER 14338/A000, U.S. Geological Service.

Bredehoeft, J. D., J. B. Wesley, and T. D. Fouch (1994), Simulations of the origin of fluid pressure, fracture generation, and the movement of fluids in the Uinta Basin, Utah, *Am. Assoc. Pet. Eng. Bull.*, *78*, 1729–1747.

Brown, A. (2000), Evaluation of possible gas microseepage mechanisms, *Am. Assoc. Pet. Geol. Bull.*, *84*, 1,775–1,789.

Cicerone, R. J., and R. S. Oremland (1988), Biogeochemical aspects of atmospheric methane, *Global Biogeochem. Cycles*, *2*, 299–327.

Cooles, G. P., A. S. Mackenzie, and T. M. Quigley (1985), Calculation of petroleum masses generated and expelled from source rocks, *Adv. Org. Geochem.*, *10*, 235–245.

Creany, S., and Q. R. Passey (1993), Recurring patterns of total organic carbon and source rock quality within a sequence stratigraphic framework, *Am. Assoc. Pet. Geol. Bull.*, *77*, 386–401.

Crutzen, P. J. (1995), On the role of CH_4 in atmospheric chemistry: Sources, sinks and possible reduction in anthropogenic sources, *Ambio*, *24*, 52–55.

Etiope, G. (2004), GEM—Geologic emissions of methane, the missing source in the atmospheric methane budget, *Atmos. Environ.*, *38*, 3099–3100, doi:10.1016/j.atmosenv.2004.04.002.

Etiope, G. (2005), Mud volcanoes and microseepage: The forgotten geophysical components of atmospheric methane budget, *Ann. Geophys.*, *48*, 1.

Etiope, G. (2009), Natural emissions of methane from geological seepage in Europe, *Atmos. Environ.*, *43*, 1430–1443, doi:10.1016/j.atmosenv.2008.03.014.

Etiope, G. (2012), Methane uncovered, *Nat. Geosci.*, *5*, 373–374, doi:10.1038/ngeo1483.

Etiope, G., and R. W. Klusman (2002), Geologic emissions of methane to the atmosphere, *Chemosphere*, *49*, 777–789, doi:10.1016/S0045-6535(02)00380-6.

Etiope, G., and R. W. Klusman (2010), Microseepage in drylands: Flux and implications in the global atmospheric source/sink budget of methane, *Global Planet. Change*, *72*, 265–274, doi:10.1016/j.gloplacha.2010.01.002.

Fouch, T. D., V. F. Nuccio, J. C. Osmond, L. MacMillan, W. B. Cashion, and C. J. Wandrey (1992), Oil and gas in uppermost Cretaceous and Tertiary rock, Uinta Basin, Utah, in *Hydrocarbon and Mineral Resources of the Uinta Basin, Utah and Colorado*, Utah Geological Association Guidebook 20, edited by T. D. Fouch, V. F. Nuccio, and T. C. Chidsey Jr., pp. 9–47, Utah Geological Association, Salt Lake City, Utah.

Fung, I., J. John, J. Lerner, E. Matthews, M. Prather, L. P. Steele, and P. J. Fraser (1991), Three-dimensional model synthesis of the global methane cycle, *J. Geophys. Res.*, *96D*, 13,033–13,065, doi:10.1029/91JD01247.

Hein, R., P. J. Crutzen, and M. Heimann (1997), An inverse modeling approach to investigate the global atmospheric methane cycle, *Global Biogeochem. Cycles*, *11*, 43–76.

Horvitz, L. (1985), Geochemical Exploration for Petroleum, *Science*, *229*, 821–827.

Johnson, R. C., and S. B. Roberts (2003) The Mesaverde total petroleum system, Uinta-Piceance Province, Utah and Colorado, Ch. 7 of *Petroleum Systems and Geologic Assessment of Oil and Gas in the Uinta-Piceance Province, Utah and Colorado*, U.S. Geological Survey Digital Data Series DDS-69-B.

Jones, V. T., and S. G. Burtell (1996), Hydrocarbon flux variations in natural and anthropogenic seeps, in *Hydrocarbon Migration and Its Near-Surface Expression*, American Association of Petroleum Geologists Memoir 66, edited by D. Schumacher and M. Abrams, pp. 203–221, AAPG Hedberg Research Conference, Vancouver, B. C.

Joye, S. B. (2012), A piece of the methane puzzle, *Nature*, *491*, 538–539, doi:10.1038/nature11749.

Kai, F. M., S. C. Tyler, J. T. Randerson, and D. R. Blake (2011), Reduced methane growth rate explained by decreased Northern Hemisphere microbial sources, *Nature*, *476*, 194–197, doi:10.1038/nature10259.

Karion, A., et al. (2013), Methane emissions estimate from airborne measurements over a western United States natural gas field, *Geophys. Res. Lett.*, *40*, 4393–4397, doi:10.1002/grl.50811.

Khalil, M. A. K., and R. A. Rasmussen (1994), Global emissions of methane during the last several centuries, *Chemosphere*, *29*, 833–842, doi:10.1016/0045-6535(94)90156-2.

Klusman, R. W. (1997), Modeling of microseepage of methane and light alkanes in the sedimentary column: Final Report to W.L. Gore & Associates, Inc.

Klusman, R. W. (2003a), Rate measurements and detection of gas microseepage to the atmosphere from an enhanced oil recovery/sequestration project, Rangely, Colorado, USA, *Appl. Geochem.*, *18*, 1825–1838, doi:10.1016/S0883-2927(03)00108-2.

Klusman, R. W. (2003b), A geochemical perspective and assessment of leakage potential for a mature carbon dioxide-enhanced oil recovery project and as a prototype for carbon dioxide sequestration; Rangely Field, Colorado, *Am. Assoc. Pet. Geol. Bull.*, *87*, 1485–1507.

Klusman, R. W., and C. J. Dick (2000), Seasonal variability in CH_4 emissions from a landfill in a cool, semiarid climate, *J. Air Waste Manage. Assoc.*, *50*, 1632–1636.

Klusman, R. W., and M. A. Saaed (1996), Comparison of light hydrocarbon microseepage mechanisms, in *AAPG Special Volumes, Memoir 66: Hydrocarbon Migration and Its Near-Surface Expression*, edited by D. Schumacher and M. A. Abrams, pp. 157–168, AAPG Hedberg Research Conference, Vancouver, B. C.

Klusman, R. W., M. E. Leopold, and M. P. LeRoy (2000), Seasonal variation in methane fluxes from sedimentary basins to the atmosphere: Results from chamber measurements and modeling of transport from deep sources, *J. Geophys. Res.*, *105D*, 24,661–24,670.

Krooss, B. M., and D. Leythaeuser (1996), Molecular diffusion of light hydrocarbons in sedimentary rocks and its role in migration and dissipation of natural gas, in *AAPG Special Volumes, Memoir 66: Hydrocarbon Migration and Its Near Surface Expression*, edited by D. Schumacher and M. A. Abrams, pp. 173–183, AAPG Hedberg Research Conference, Vancouver, B. C.

Kvenvolden, K. A., and B. W. Rogers (2005), Gaia's breath—Global methane exhalations, *Mar. Pet. Geol.*, *22*, 579–590, doi:10.1016/j.marpetgeo.2004.08.004.

Kvenvolden, K. A., T. D. Lorenson, and W. S. Reeburgh (2001), Attention turns to naturally occurring methane seepage, *EOS Trans., Am. Geophys. Union*, *82*(40), 457.

Lassey, K. R., D. C. Lowe, and A. M. Smith (2007), The atmospheric cycling of radiomethane and the "fossil fraction" of the methane source, *Atmos. Chem. Phys.*, *7*, 2141–2149.

Law, B. E. (1984), Relationships of source-rock, thermal maturity, and overpressuring to gas generation and occurrence in low-permeability Upper Cretaceous and lower Tertiary rocks, greater Green River Basin, Wyoming, Colorado, and Utah, in *Hydrocarbon Source Rocks of the Greater Rocky Mountain Region*, pp. 469–490, Rocky Mountain Association of Geologists, Denver, Colo.

Lelieveld, J., P. J. Crutzen, and F. D. Dentener (1998), Changing concentration, lifetime and climate forcing of atmospheric methane, *Tellus B*, *50*, 128–150.

Leythaeuser, D., R. G. Schaefer, and A. Yukler (1982), Role of diffusion in primary migration of hydrocarbons, *Am. Assoc. Pet. Geol. Bull.*, *66*, 408–429.

Lowe, D. C., C. A. M. Brenninkmeijer, M. R. Manning, R. Sparks, and G. Wallace (1988), Radiocarbon determination of atmospheric methane at Baring Head, New Zealand, *Nature*, *332*, 522–525.

Lyman, S., and H. Shorthill (2013), Final report: 2012 Uintah Basin winter ozone and air quality study, Utah State University, Document No. CRD13-320.32. [Available at rd.usu.edu/files/uploads/ubos_2011-12_final_report.pdf.]

MacGowan, D. B., D. R. Britton, F. P. Miknis, and R. C. Surdam (1992), Organic geochemistry and maturation trends of shales and coals, almond formation, Mesaverde Group, greater Green River Basin, Wyoming: A comparison with laboratory maturation of almond coals by hydrous pyrolysis, in *Rediscover the Rockies*, 43rd Annual Field Conference Guidebook, pp. 221–236, Wyoming Geological Association, Casper, Wyoming.

Martin, R., K. Moore, M. Mansfield, S. Hill, K. Harper, and H. Shorthill (2011), Final report: Uinta Basin winter ozone and air quality study: December 2010–March 2011, Document Number EDL/11-039, Energy Dynamics Laboratory, Utah State University Research Foundation, Logan, Utah. [Available at rd.usu.edu/files/uploads/edl_2010-11_report_ozone_final.pdf.]

McPherson, B. J. O. L. (1996), A three-dimensional model of the geologic and hydrodynamic history of the Uinta Basin, Utah: Analysis of overpressures and oil migration, PhD dissertation, University of Utah.

McPherson, B. J. O. L., and J. D. Bredehoeft (2001), Overpressures in the Uinta Basin, Utah: Analysis using a three-dimensional basin evolution model, *Water Resour. Res.*, *37*, 857–871, doi:10.1029/2000WR900260.

Milkov, A. V. (2011), Wordwide distribution and significance of secondary microbial methane formed during petroleum biodegradation in conventional reservoirs, *Org. Geochem.*, *42*, 184–207, doi:10.1016/j.orggeochem.2010.12.003.

Milucka, J., T. G. Ferdelman, L. Polerecky, D. Franzke, G. Wegener, M. Schmid, I. Lieberwirth, M. Wagner, F. Widdel, and M. M. M. Kuypers (2012), Zero-valent sulphur is a key intermediate in marine methane oxidation, *Nature*, *491*, 541–546, doi:10.1038/nature11656.

Neef, L., M. van Weele, and P. van Velthoven (2010), Optimal estimation of the present-day global methane budget, *Global Biogeochem. Cycles*, *24*, GB4024, doi:10.1029/2009GB003661.

Neuzil, C. E. (1995), Abnormal pressures as hydrodynamic phenomena, *Am. J. Sci.*, *295*, 742–786.

Nuccio, V. F., and L. N. R. Roberts (2003), Thermal maturity and oil and gas generation history of petroleum systems in the Uinta-Piceance Province, Utah and Colorado, in *Petroleum Systems and Geologic Assessment of Oil and Gas in the Uinta-Piceance Province, Utah and Colorado*, U.S. Geological Survey Digital Data Series DD5-69-B, Central Region, Denver, Colo.

Nuccio, V. F., J. W. Schmoker, and T. D. Fouch (1992), Thermal maturity, porosity, and lithofacies relationships applied to gas generation and production in Cretaceous and Tertiary low-permeability (tight) sandstones, Uinta Basin, Utah, in *Hydrocarbon and Mineral Resources of the Uinta Basin, Utah and Colorado: Utah Geological Association Guidebook 20*, edited by T. D. Fouch, V. F. Nuccio, and T. C. Chidsey Jr., pp. 77–93, Utah Geological Association, Salt Lake City, Utah.

Op den Camp, H. J. M., T. Islam, M. B. Stott, H. R. Harhangi, A. Hynes, S. Schouten, M. S. M. Jetten, N.-K. Birkeland, A. Pol, and P. F. Dunfield (2009), Environmental, genomic and taxonomic perspectives on methanotrophic *Verrucomicrobia*, *Environ. Microbiol. Rep.*, *1*, 293–306, doi:10.1111/j.1758-2229.2009.00022.x.

Peischl, J., et al. (2013), Quantifying sources of methane using light alkanes in the Los Angeles basin, California, *J. Geophys. Res. Atmos.*, *118*, 4974–4990, doi:10.1002/jgrd.50413.

Pepper, A. S., and P. J. Corvi (1995a), Simple kinetic models of petroleum formation. Part I: Oil and gas generation from kerogen, *Mar. Pet. Geol.*, *12*, 291–319.

Pepper, A. S., and P. J. Corvi (1995b), Simple kinetic models of petroleum formation. Part III: Modelling an open system, *Mar. Pet. Geol.*, *12*, 417–452.
Pepper, A. S., and T. A. Dodd (1995), Simple kinetic models of petroleum formation. Part II: oil-gas cracking, *Mar. Pet. Geol.*, *12*, 321–340.
Pétron, G., et al. (2012), Hydrocarbon emissions characterization in the Colorado Front Range: A pilot study, *J. Geophys. Res.*, *117*, D04304, doi:10.1029/2011JD016360.
Price, L. C. (1986), A critical review and proposed working model of surface geochemical exploration, in *Unconventional Methods in Exploration for Petroleum and Natural Gas IV*, edited by M. J. Davidson, pp. 245–304, Southern Methodist Univ. Press, Dallas, Tex.
Quick, J. C. and R. Ressetar (2012), Thermal maturity of the Mancos Shale within the Uinta Basin, Utah and Colorado, American Association of Petroleum Geologists, Annual Convention and Exhibition, Long Beach, Calif., 22–25 April. [Available at http://geology.utah.gov/emp/shalegas/cret_shalegas/index.htm.]
Ressetar, R. (2012), Executive summary. [Available at http://geology.utah.gov/emp/shalegas/cret_shalegas/index.htm.]
Sachs, W. (1998), The diffusional transport of methane in liquid water: Method and result of experimental investigation at elevated pressure, *J. Pet. Sci. Eng.*, *21*, 153–164, doi:10.1016/S0920-4105(98)00048-5.
Saunders, D. F., K. R. Burson, and C. K. Thompson (1999), Model for hydrocarbon microseepage and related near-surface alterations, *Am. Assoc. Pet. Geol. Bull.*, *83*, 170–185.
Schamel, S. (2005), Shale gas reservoirs of Utah: Survey of an unexploited potential energy resource, *Open File Rep., 461*, Utah Geological Survey, Utah Division of Natural Resources, Salt Lake City, Utah.
Schamel, S. (2006), Shale gas resources of Utah: Assessment of previously undeveloped gas discoveries, *Open File Rep. 499*, Utah Geological Survey, Utah Division of Natural Resources, Salt Lake City, Utah.
Schlömer, S., and B. M. Krooss (1997), Experimental characterisation of the hydrocarbon sealing efficiency of cap rocks, *Mar. Pet. Geol.*, *14*, 565–580.
Schnell, R. C., S. J. Oltmans, R. R. Neely, M. S. Endres, J. V. Molenar, and A. B. White (2009), Rapid photochemical production at high concentrations in a rural site during winter, *Nat. Geosci.*, *2*, 120–122, doi:10.1038/ngeo415.
Simpson, I. S., M. P. S. Andersen, S. Meinardi, L. Bruhwiler, N. J. Blake, D. Helmig, F. S. Rowland, and D. R. Blake (2012), Long-term decline of global atmospheric ethane concentrations and implications for methane, *Nature*, *488*, 490–494, doi:10.1038/nature11342.
Spencer, C. W. (1987), Hydrocarbon generation as a mechanism for overpressuring in Rocky Mountain Region, *Am. Assoc. Pet. Geol. Bull.*, *71*, 368–388.
Spencer, C. W. (1995) Uinta-Piceance Basin Province (020), Energy Resources Program, National Oil and Gas Assessment, U.S. Geological Survey.
Stern, D. I., and R. K. Kaufmann (1996), Estimates of global anthropogenic methane emissions 1860–1993, *Chemosphere*, *33*, 159–176, doi:10.1016/0045-6535(96)00157-9.
Stoeckenius, T., and L. Ma (2010), Final report: A conceptual model of winter ozone episodes in Southwest Wyoming, Environ, Novato, CA.
Tedesco, S. A. (1999), Anomaly shifts indicate rapid surface seep rates, *Oil Gas J.*, *97*(13), 69–72.
Tissot, B. P., and D. H. Welte (1984), *Petroleum Formation and Occurrence*, 2nd ed., Springer-Verlag, New York.
Tissot, B., G. Deroo, and A. Hood (1978), Geochemical study of the Uinta Basin: Formation of petroleum from the Green River formation, *Geochim. Cosmochim. Acta*, *42*, 1469–1485.
Utah Division of Oil, Gas, and Mining (UDOGM) (2013), LiveData Search. [Available at oilgas.ogm.utah.gov.]
Vandenbroucke, M., and C. Largeau (2007), Kerogen origin, evolution, and structure, *Org. Geochem.*, *38*, 719–833, doi:10.1016/j.orggeochem.2007.01.001.
Wahlen, M., N. Tanaka, R. Henry, B. Deck, J. Zeglen, J. S. Vogel, J. Southon, A. Shemesh, R. Fairbanks, and W. Broecker (1989), Carbon-14 in methane sources and in atmospheric methane: The contribution from fossil fuel carbon, *Science*, *245*, 286–290.
White, J. W. C., D. F. Ferretti, J. B. Miller, D. M. Etheridge, K. R. Lassey, D. C. Lowe, C. M. MacFarling, M. F. Dreier, C. M. Trudinger, and T. van Ommen (2007), The global methane budget over the last 2000 years: $^{13}CH_4$ reveals hidden information, in *Stable Isotopes as Indicators of Ecological Change*, edited by T. E. Dawson and R. T. W. Siegwolf, pp. 235–248, Elsevier, Oxford.
Wiggins, W. D., and P. M. Harris (1994), Lithofacies, depositional cycles, and stratigraphy of the lower Green River Formation, Southwestern Uinta Basin, Utah, in *Lacustrine Reservoir and Depositional Systems*, pp. 105–141, Society for Sedimentary Geology, Tulsa, Okla.
Witherspoon, P. A., and D. N. Saraf (1965), Diffusion of methane, ethane, propane, and n-butane in water from 25 to 43°C, *J. Phys. Chem.*, *69*, 3752–3755.
Zhang, Y., C. W. Gable, G. A. Zyvoloski, and L. M. Walter (2009), Hydrogeochemistry and gas compositions of the Uinta Basin: A regional-scale overview, *Am. Assoc. Pet. Geol. Bull.*, *93*, 1087–1118, doi:10.1306/05140909004.
Zhang, Y., B.-Z. Li, J.-S. Yang, S.-Q. Wang, and H.-L. Yuan (2012), Diversity of culturable butane-oxidizing bacteria in oil and gas field soil, *Huanjing Kexue/Environ. Sci.*, *33*, 299–304.